Integrated optical silicon IC compatible nanodevices for biosensing applications

L. M. Lechuga[1], B. Sepúlveda[1], A. Llobera[2], A. Calle[1] and C. Domínguez[2]

Biosensors Group. Microelectronics National Center (CNM). CSIC. Spain.
[1]IMM. Isaac Newton, 8 - 28760 Tres Cantos, Madrid [2]IMB. Campus UAB - 08193 Bellaterra, Barcelona

ABSTRACT

We present a nanobiosensor device based on evanescent wave detection by using optical waveguides in a highly sensitive interferometric configuration. The device is fabricated by standard CMOS microelectronics technology after a precise design of the device structure in order to achieve a high surface sensitivity for biosensing applications. Direct immunosensing with the sensor has been tested after a covalent bonding of the receptor layer to the surface device. A flow delivery system, optical bench for testing, data acquisition and processing of the signal have been also implemented.

Keywords: Biosensor, Integrated optics, Mach-Zehnder interferometer, Silicon microtechnology, optical waveguides.

1. INTRODUCTION

Integrated optical devices are increasingly been used as specific chemical sensors and biosensors. It becomes clear that this technology can be a serious alternative to conventional assays techniques because they can avoid expensive, complex and time consuming procedures[1]. In general, integrated optical sensors make use of the evanescent field detection principle (Fig.1). These evanescent wave sensors show a great potential for sensing biomolecular interactions, allowing real-time analysis without labeling requirements.

All these sensors make use of optical waveguides as the basic element of their structure for light propagation and are based on the same operation principle. The evanescent field is the part of the guided light that travels through a region that extends outward, around a hundred of nanometers, into the media surrounding the waveguide. When there is a change in the optical characteristics of the outer medium (i.e. refractive index change or a biochemical reaction), a modification in the optical properties of the guided wave (phase velocity) is induced via the evanescent field. Optical evanescent wave biosensing techniques, allow the direct monitoring of small changes in the optical properties and are particularly useful in the direct affinity detection of biomolecular interaction as they can record the binding and dissociation in real time. The direct detection method is not as sensitive as indirect ones (i.e. fluorescence, radiolabeling or enzyme amplification) but it requires, generally, no prior sample preparation and can be use in real time evaluations allowing the determination of concentration, kinetic constants and binding specificity of biomolecules.
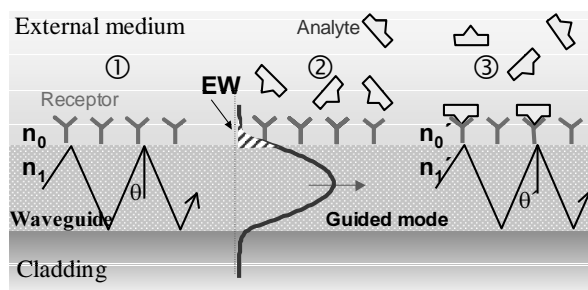

Fig. 1. Biomolecular interaction sensing by the evanescent wave detection principle in an optical waveguide sensor

There is a great variety of optical methods that can be employed for the detection but those which can give a direct signal after a molecular interaction (without the use of labels) have attracted quite attention, as for example Surface Plasmon Resonance[2], Grating Coupler[3], Resonant Mirror[4] or Interferometers[5,6] . Interferometric biosensors arrangement is highly sensitive and is the only one that provides with an internal reference for compensation of refractive-index fluctuations and unspecific adsorption. Interferometric sensors have a broader dynamic range than most other types of sensors and show higher sensitivity as compared to other integrated scheme as it is shown in Table 1, where a comparison of the different sensor technologies as a function of the limit of detection (in pg/mm^2) is presented[7].

Due to the high sensitivity of the interferometer sensor the direct detection of small molecules (as for example environmental pollutants where concentrations down to 0.1 ng/ml must be detected) would be possible with this device. Detection limit is generally limited by electronic and mechanical noise, thermal drift, light source instabilities and chemical noise. But the intrinsic reference channel of the interferometric devices offers the possibility of reducing common mode effects like temperature drifts and non-specific adsorptions. Detection limit of 10^{-7} in refractive index (or better) can be achieved with these devices[8] which opens the possibility of development of highly sensitive devices for in-situ pollutant detection. Several interferometric devices have been described as the difference interferometer, the Mach-Zehnder or the Young interferometer[7].

Table 1. Comparison of sensitivities for different integrated optical biosensors

Sensing principle	Limit of detection (pg/mm^2)
SPR	2-5
Waveguide-SPR	2
Resonant Mirror	5
Grating Coupler	1-10
Mach-Zehnder Interferometer	0.1
Differential Mode Interferometer	1
Young Interferometer	0.7
Reflectometric interference Spectroscopy (RifS)	1-5

The type of interferometer that is most employed for biosensing is the Mach-Zehnder device. A theoretical study shows that the Mach-Zehnder interferometer sensor seems to be one of the more promising concepts[9] for detection of low concentration of small molecules without labels (10^{-12} M or even lower). The main problem in the development and possible commercialization of the MZI device is the complexity of the design, fabrication and optical adjustments: the overall procedure for MZI fabrication is rather laborious and monomode waveguides are required increasing, even more, the complexity of the technology. But the utilization of microtechnology for the integration of these devices offers some advantages as better control of the light path by the use of optical waveguides, mechanical stability, higher sensitivity, miniaturization and the possibility of mass-production.

For evaluation of specific interactions, the receptor is covalently attached to the sensor surface, while the complementary molecule binds to the receptor from free solution. The recognition of the complementary molecule by the receptor causes a change in the refractive index and the sensor monitors that change. After the molecular interaction, the surface can be regenerated using a suitable reagent in order to remove the bound analyte without denaturing the immobilized receptor. An extensive range of analytes can be detected using evanescent principle without labeling requirements, from hormone disrupters, proteins, DNA, viruses to pesticides. A large number of applications for these sensors ranges from clinical, industrial control processes, functional genomics, proteomics, veterinary field to food industry or environmental monitoring[10].

The integrated nanosensor that we have developed has a symmetric channel waveguide Mach-Zehnder interferometer configuration and has been designed for having a high sensitivity towards biochemical interactions. The device has been fabricated by standard silicon technology using a CMOS compatible process. The guiding layer consists of a ridge

structure of silicon nitride with a thickness of 200 nm, a width of 4 μm and a rib of 4 nm. The nanodevice has been employed for biosensing evaluations.

2. PRINCIPLE OF OPERATION OF INTERFEROMETRIC SENSORS

2.1. Integrated Mach-Zehnder Interferometer

In the integrated interferometric arrangement (see Figure 2) two light beams of equal intensity are made to travel across two areas of a waveguide (one is the sensor and the other is the reference) and finally they are combined, creating an interference pattern of dark and light fringes[7]. When a chemical or biochemical reaction takes place in the sensor area, only the light that travels through this arm will experience a change in its effective refractive index. At the sensor output, the intensity (I) of the light coming from both arms will interfere, showing a sinusoidal variation that depends on the difference of the effective refractive indexes of the sensor and reference arms (ΔN) and on the interaction length (L):

$$I \propto \left[1 + V \cdot \cos \Delta \Phi \right] \tag{1}$$

where V is the visibility factor and $\Delta \Phi = \left(\Phi_r - \Phi_s \right)$ is the phase shift between guided modes in the reference and sensing arm:

$$\Delta \Phi = \frac{2\pi}{\lambda} \cdot L \cdot \Delta N \tag{2}$$

Where λ is the wavelength. This sinusoidal variation can be directly related to the concentration of the analyte to be measured. The visibility factor gives the contrast of the interference signal (difference between the maximum and minimum intensity) and depends on the coupling factor of the divisor and on the propagation losses of the guided mode in the interferometer arms. To obtain a maximum visibility factor it is important to design a divisor or Y-junction with a coupling factor of 3 dB, that is, input light is equally divided in each branch of the interferometer. Moreover, propagation losses in the sensor and reference arm should be identical.
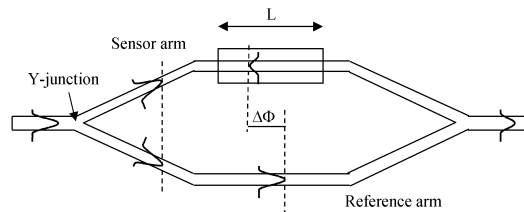

Fig. 2. Mach-Zehnder interferometer configuration

To obtain an efficient transducer for detecting molecular interactions, the optical waveguides of the interferomer must verify two main conditions: a **Monomode behaviour** and a **high Surface Sensitivity.**

2.2 High surface sensitivity

For sensing purposes, the optical waveguide may be designed to assure high surface sensitivity, which means that the sensor response for changes in the optical properties of the outer medium must be as high as possible. Surface sensitivity for processes that involve the adsorption of molecules is defined as the rate of change of the effective refractive index of the guided mode, N, as the thickness of the homogeneous molecular adlayer, d_l, varies[11,12]. This sensitivity is related to the squared field magnitude of the guide mode at the core-outer medium interface, considering a homogeneous adsorbed layer of refractive index n_0 and thickness d_l. Surface sensitivity can be expressed as a function of the power fraction in the evanescent field:

$$S_{\mathrm{sup}} \equiv \frac{\partial N}{\partial d_\ell} \approx \frac{\gamma_o}{N} \cdot \left[\left(\frac{n_\ell}{n_o} \right)^{2\rho} \gamma_o^2 - \left(\frac{n_o}{n_\ell} \right)^{2\rho} \gamma_\ell^2 \right] \cdot \frac{P_o}{P_T} \qquad (3)$$

with $\gamma_i = k_o \sqrt{N^2 - n_i^2}$ (i = o, l), where n_o is the refractive index of the outer medium, n_l is the refractive index of adsorbed layer, N is the effective refractive index of the guided mode, P_0/P_T is the power fraction of the guided mode at the cover medium and ρ is 0 for TE mode and 1 for TM mode.

Therefore, for sensing applications the strength and distribution of the evanescent field in the outer medium need to be maximized in order to assure a high response. For that, the thickness and refractive indices of the waveguide layers must be designed in such a way that a large fraction of the guided mode travels through the outer medium. For TIR waveguides, maximum surface sensitivity is achieved for high refractive index contrast and core thickness of hundreds of nanometers[11]. Up to now, the sensor with highest surface sensitivity developed is based on interferometric arrangement fabricated using microelectronics technology[9], with a core refractive index and thickness of 2.00 and 100 nm, respectively. The corresponding value of the theoretical sensitivity for this structure is $S_s = 3.4 \cdot 10^{-4}$ nm^{-1} for TE polarization.

2.3 Monomode behavior

Due to the evanescent sensing approach employed by the sensors, the optical waveguides must be monomode. If several modes were propagated through the structure, each of them would detect the variations in the characteristics of the outer medium and the information carried by all the modes would interfere between them. To theoretically evaluate this characteristic, we have developed a home-made one-dimensional computational program based on the Non-Uniform finite difference method. In channel waveguides, monomode behaviour depends on the core thickness, on the width and depth of the channel and on the difference between the core and cladding refractive indices (index contrast $\Delta n = \left(n_c^2 - n_s^2 \right) / n_c^2$).

If the difference of the core-cladding refractive index is large (Δn higher than 10%), monomode behaviour is achieved with core thickness of hundreds of nanometers. The cladding thickness can be of only a few micrometers due to the small penetration of the evanescent field into the cladding. However, the rib depth must be around several nanometers for single-mode waveguides for a TIR waveguide with a core thickness $d_c = 280$ nm and index contrast $\Delta n = 40\%$. Due to the nanometer dimensions of the core thickness, insertion losses for direct coupling of light with commercial optical fibers (core size between 4 and 10 μm, depending on the design wavelength) are high. Then, assuming a fixed wavelength, the monomode behavior can be controlled with a proper design of the thickness and refractive indexes of the waveguide layers.
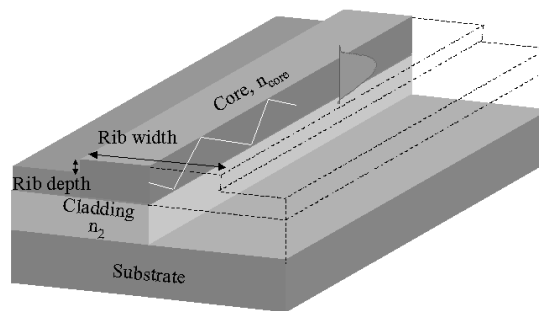

Fig. 3. Three dimensional view of TIR waveguides configuration to be used for the MZI sensor

2.4. MZI sensor configuration

Summarising the previous results, for the design of TIR structures for sensor applications, we must come to an agreement between single-mode behaviour, low attenuation losses for the fundamental mode and high surface sensitivity. For those reasons, the structure that has been finally chosen, for an operating wavelength of 0.633 µm, has the following structure: Silicon substrate; a 2 µm thick silicon dioxide cladding (n=1.46) and a silicon nitride core layer with a refractive index of 2.00 and thickness of 250 nm. To obtain a maximum visibility factor the MZI configuration was designed where the Y-junction is shaped with circular bend with radii of 80 mm. The separation between the sensor and reference arms is of 100 µm to avoid coupling between modes travelling through both branches.

3. FABRICATION OF THE SENSOR

The devices are fabricated in our Clean Room facilities using a Silicon CMOS compatible process. The waveguide substrate is Silicon (n_s=3.85-j0.019 at the working wavelength of 632.8 nm). The cladding is a thermally grown silicon dioxide (SiO2) layer with a refractive index of 1.46 and a thickness of 2 µm. The waveguide core is a silicon nitride (Si_3N_4) layer with a thickness of 250 nm and a refractive index of 2.00 deposited by Low Pressure Chemical Vapor Deposition (LPCVD) at 800 ºC. To obtain monomode lateral confinement of light, a rib structure is defined. The rib depth is 4 nm in order to assure monomode propagation. The rib is defined on the core layer by Reactive Ion Etching (RIE). Several devices were designed with different widths, ranging from 4 to 7 µm, to experimentally analyse its influence in the guiding properties of the structure. The sensing process (change in the optical properties of the outer medium) will take place during a certain distance, L, in the sensor arm of the interferometer. For that reason, the rest of the MZI is protected from the environment with a covering layer and the sensing window of length L is opened in one of the interferometer branches. The protective layer is a silicon oxide layer with a refractive index of 1.46 deposited by PECVD at 300 ºC. The thickness of this layer is 2 µm, enough to isolate the core from the environment. The opening of the sensor area in the protective layer is done, after a photolitographic process, by chemical etching with a HF:H4NF (1:7) solution. The sensor area has a width of 100 µm and a length of 10 mm. Finally the sensors are cut in individual pieces and polished for light coupling by end-face. The total length of the sensor is 35 mm. The final structure is shown in Fig. 3.
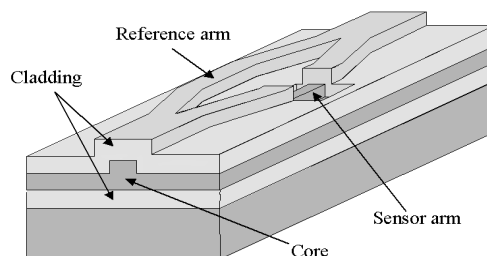

Fig.3. Cross Section of one MZI device

4. OPTICAL CHARACTERISATION

The optical characterisation (see Fig 4) is performed with TE-polarised light from a He-Ne laser (λ=0.633 µm) that is coupled to a single-mode optical fibre (3.8 µm core diameter) using a microscope objective (40x). The optical fibre has a small length (around 15 cm) and is placed in straight line to preserve the input TE-polarisation. The end of the mono-mode fibre is placed in front of the waveguide rib face to couple light into the sensor structure (end-fire coupling). Light is collected by a multi-mode standard optical fibre (50 µm core diameter) connected to a silicon photodiode. Precise translation stages are used for the accurate alignment of all the components. A synchronous detection scheme is used with the aid of a lock-in amplifier and a light chopper. Finally, homemade software is available for collecting the measurement data.
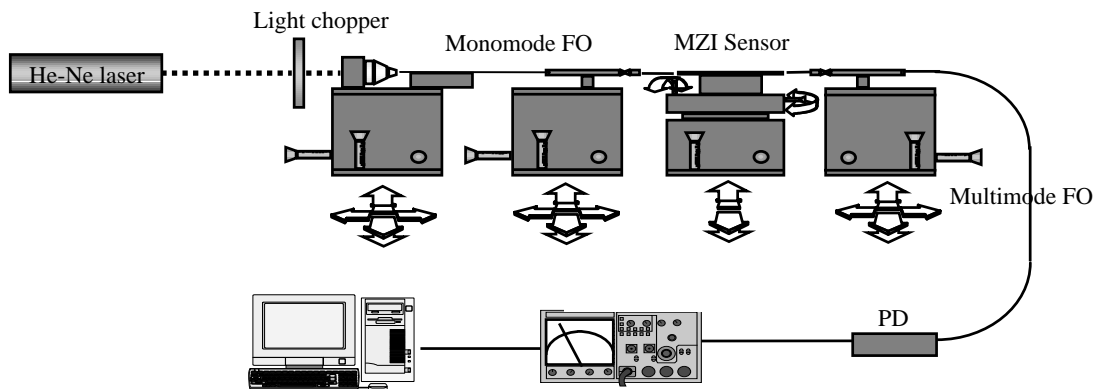
Fig. 4. Optical bench for MZI nanodevice optical and biochemical characterisation

An experimental study was made to analyse the guiding conditions of the fabricated structures. Straight waveguides and Y-couplers were used to measure the propagation losses and modal behaviour as a function of the waveguide width and the polarization. Propagation losses, measured by the Fabry-Perot resonance method [13], vary between 0.15-0.25 dB/cm for TE polarization and between 0.2-0.35 dB/cm for TM polarization. Monomodal behaviour is observed for the devices with 4 μm of rib width. For wider waveguides a second propagating mode could be excited. With these results we can conclude that the optimum interferometers for sensing applications should have a rib width of 4 μm to assure monomode behaviour, while low losses are assured with couplers designed with circular arms of R = 80 mm.
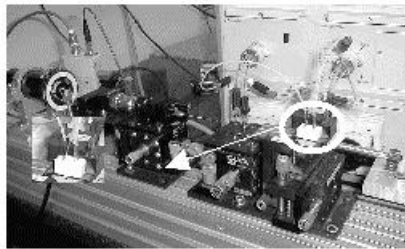

Fig 5. Photograph of the experimental set-up showing ythe flow cell and the automatic flow injection delivery system employed for the measurements.

5. BIOSENSING APPLICATIONS

The sensor is being developed for the detection of biochemical interactions between a receptor molecule and its complementary analyte. The effect of this reaction is comparable to a change of the bulk refractive index of the outer medium. Therefore, the use of solutions with different refractive indexes is useful for studying the sensor sensitivity. Several solutions were prepared with different glucose concentrations in water, with refractive indexes varying from 1.3325 to 1.4004 (=0.0002), as determined by an Abbe refractometer operating at 25ºC. A flow cell mechanized in Teflon (with a channel width of 3 mm, a depth of 100 μm and a length of 15 mm) is clamped onto the interferometer and a flow injection system is used to deliver the glucose solutions into the sensor area. In Figure 5 a photograph of the experimental set-up with the flow cell used for the measurements is shown.

The different glucose solutions with varying refractive indexes were introduced alternatively,. With these measurements, a calibrating curve was evaluated where the phase response of the sensor is plotted versus the variation in the refractive index as is depicted in Fig. 6. The lower detection limit measured was $\Delta n_{o,min} = 7 \times 10^{-6}$ that means an effective refractive index of $\Delta N = 4 \cdot 10^{-7}$. The detection limit has been estimated measuring the signal-to-noise ratio (around 20 dB) and considering the most favourable case in which the interferometer is located at its quadrature point. Under this conditions, we estimate that the lowest phase shift measurable would be around $0.01 \cdot 2\pi$. The detection limit

value corresponds to a surface sensitivity around 2×10^{-4} nm^{-1}, close to the maximum surface sensitivity reported up to now.
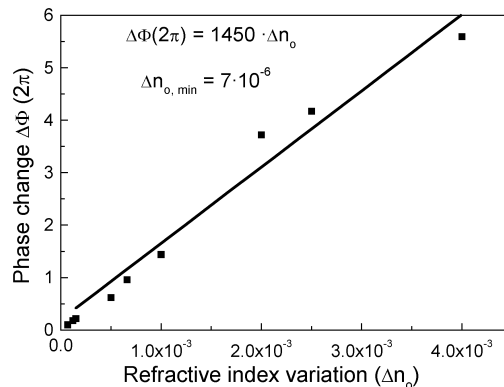

Fig. 6. Sensitivity evaluation of the TIR-MZI nanodevice by using glucose solutions of varying refractive indices.

The sensor described in this work has been applied to the detection of the insecticide carbaryl. Carbaryl is an N-methylcarbamate pesticide extensively used as a broad-spectrum insecticide. The immunoassays developed to monitor this pollutant require the use of three different components. The critical part is the monoclonal antibody (LIB-CNH45 Mab), since it is responsible for the sensitivity and specificity of the analyte to determine. The second component is the analyte (antigen) to detect, which is unable to produce directly an immune response due to its low molecular weight (~200D). Therefore, it is necessary to design the third compound: the hapten, that can be covalently bind to a large carrier, usually a protein. A hapten is a derivative of the analyte, in this case carbaryl, with similar geometry and structure, which contains an appropriate group (COOH, -NH$_2$) for attachment to the carrier protein (OVA). Once the hapten-carrier conjugate has been formed, antibodies can be produced by animal immunization. To achieve higher specificity and lower cross-reactivity, monoclonal antibodies, obtained unlimitedly by the hybridoma technique are preferred to heterogeneous polyclonal antibodies.
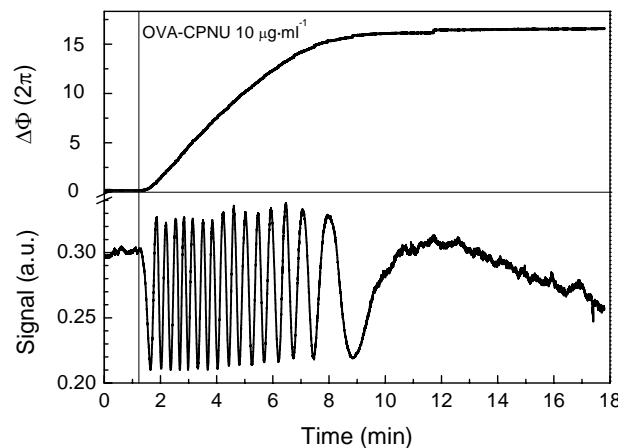

Fig.7. Immobilization of the receptor at nanometer scale by covalent attachment

Carbaryl determination with this technique, requires the immobilization of the hapten-carrier conjugate (carbaryl OVA-CPNU) and the subsequent addition of the antibody LIB-CNH45. The reproducibility and regeneration of the sensor surface requires the application of a defined immobilization procedure, and then the sensor surface may be prepared to attach covalently the receptor. The immobilization procedure used is an esterification process of the silicon nitride sensor surface that allow to bind covalently, at nanometer scale, the receptor molecules. A concentration of 10

μg·ml^{-1} in a buffer solution (PBST, *Phosphate Buffered Saline Tween*) with pH 7 at a constant flow rate of 20 μl·min^{-1} is introduced. As it is observed in Figure 7 the phase change, in the first part of the process, is fast and as the surface is being progressively occupied, the phase response $\Delta\Phi$ varies more slowly. The total phase change is 16.2×2π, that corresponds to the adsorption of a homogeneous antigen monolayer of average thickness $d_\ell \approx 3.2$ nm (surface covering of 1.9 ng·mm^{-2}). A concentration of 10 μg·ml^{-1} of the antibody (LIB-CNH45) is flowed through the sensor, giving an additional phase change of $\Delta\Phi = 5\times2\pi$ due to the immunoreaction as it is shown in Figure 8. After rinsing with PBST, the antibodies that have not reacted are washed out, being the net sensor response of $\Delta\Phi = 0.4\times2\pi$ (surface covering of 0.33 ng·mm^{-2})
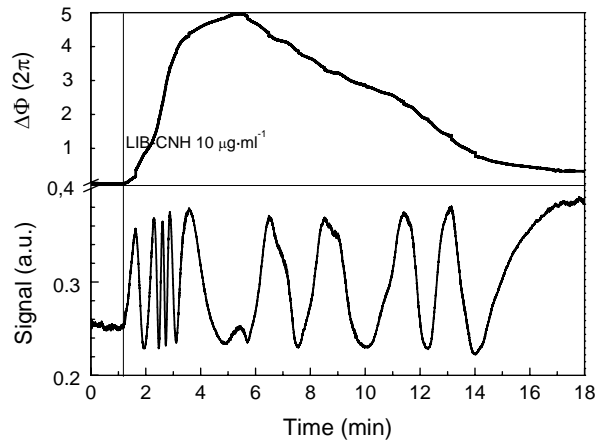

Fig.8. Immunoreaction with the pollutant.

6. CONCLUSIONS

We have developed an optical nanosensor based on Silicon microelectronics technology. It makes use of an integrated MZI configuration fabricated with TIR waveguides. The main features of these waveguides must be monomode behaviour and high surface sensitivity. The small dimensions of the core thickness (hundreds of nanometers) assures high surface sensitivity, while to obtain monomode behaviour, the parameters of the waveguide must be carefully chosen. We have presented experimental results of a MZI nanosensor working as a refractometer and as biosensor. For the MZI-TIR sensor the lower refractive index detection limit $\Delta n_{o,min} = 7\times10^{-6}$. Finally, we present measurements of the sensor for the detection of an environmental pollutant.

ACKNOWLEDGMENTS

REFERENCES

1. Kooyman, R.P.H. & Lechuga, L.M., "Immunosensors based on Total Internal Reflectance", Ch. 8, *Handbook of Biosensors: Medicine, Food and the Environment*, ed. E. Kress-Rogers, CRC Press, Florida (USA), pp. 169-196, 1997.
2. J. Homola, S.S. Yee and G. Gauglitz. "Surface plasmon resonance sensors: review". Sens. Act. B, 54 (1999) 3-15.
3. M. Wiki, H. Gao, M. Juvet and R.E. Kunz. "Compact integrated optical sensor system". Biosens. Bioelec. 16 (2001) 37-45

4. T. Kinning and P. Edwards. "The resonant mirror optical biosensor", Ch. 8 In *Optical Biosensors: present and future.* Ed. F.S. Ligler and C.A. Rowe Taitt. Elsevier, NL (2002).

5. B.H. Scheider, E.L. Dickinson, M.D. Vach, J.V. Hoijer and L.V. Howard. "Optical chip immunoassay for hCG in human whole blood". Biosens. Bioelec. 15 (2000) 597-604.

6. A. Bramdenburg, R. Krauter, C. Künzel, M. Stefan and H. Schulte. "Interferometric sensor for detection of surface-bound bioreactions". Applied Optics, 39 (34) (2000) 6396-6405.

7. L. M. Lechuga, F. Prieto and B. Sepúlveda. *Interferometric Biosensors for environmental pollution detection.* In Optical Sensors for industrial and environmental applications. Ed. R. Narayanaswamy and O.S. Wolfbeis. Springer *(In Press).*

8. Lechuga, L.M., Lenferink, A.T.M., Kooyman, R.P.H. & Greve, J., "Feasibility of Evanescent Wave Interferometer Immunosensors for Direct Detection of Pesticides: Chemical Aspects", *Sensors and Actuators B*, **24**-**25**, pp. 762, 1995.

9. E.F. Shipper, A.M. Brugman, C. Domínguez , Lechuga, L.M, Kooyman, R.P.H. & Greve, J., "The realization of an integrated Mach-Zehnder waveguide immunosensor in silicon technology" *Sensors and Actuators B*, vol. 40, pp. 147-153, 1997.

10. *Commercial Biosensors: applications to clinical, bioprocess and the environmental samples.* Ed G. Ramsay. John Wiley & Sons, INC. Richmong, Virginia, USA (1998).

11. K. Tiefenthaler, W. Lukosz, "Sensitivity of grating couplers as integrated-optical chemical sensors," *J. Opt. Soc. Am. B*, vol. 6, pp. 209-220, 1989.

12. O. Parriaux, G.J. Veldhuis, "Normalized analysis for the sensitivity optimization of integrated optical evanescent-wave sensors," *J. Lightwave Technol.,* vol. 16, pp. 573-582, 1998.